Supplementary Information

Two-Dimensional Palladium Diselenide for Oxygen Reduction Reaction

See Wee Koh[1],† Jie Hu[1,2],† Jeemin Hwang[3],† Peng Yu[4],† Zixu Sun[1], Qiunan Liu[5], Wei Hong[1], Junyu Ge[1], Jipeng Fei[1], Byungchan Han[3],* Zheng Liu[6],* Hong Li[1,7,8*]

[1]School of Mechanical and Aerospace Engineering, Nanyang Technological University, 639798, Singapore
[2]State Key Laboratory of Metastable Materials Science and Technology, Yanshan University, Qinhuangdao 066004, P. R. China.
[3]Department of Chemical and Biomolecular Engineering, Yonsei University, Seoul 03722, Republic of Korea
[4]State Key Laboratory of Optoelectronic Materials and Technologies, School of Materials Science and Engineering, Sun Yat-sen University, Guangzhou 510275, People's Republic of China.
[5]Nano Energy Center, State Key Laboratory of Metastable Materials Science and Technology, Yanshan University, Qinhuangdao 066004, P. R. China
[6]School of Material Sciences and Engineering, Nanyang Technological University, 639798, Singapore
[7]CINTRA CNRS/NTU/THALES, UMI 3288, Research Techno Plaza, 637553, Singapore
[8]Centre for Micro-/Nano-electronics (NOVITAS), School of Electrical and Electronic Engineering, Nanyang Technological University, 639798, Singapore

*corresponding authors. E-mail: bchan@yonsei.ac.kr; z.liu@ntu.edu.sg; ehongli@ntu.edu.sg

†These authors contributed equally to this work.

Key words: two-dimensional catalyst, palladium diselenide, electrochemical intercalation, oxygen reduction, selenium vacancy, DFT calculation

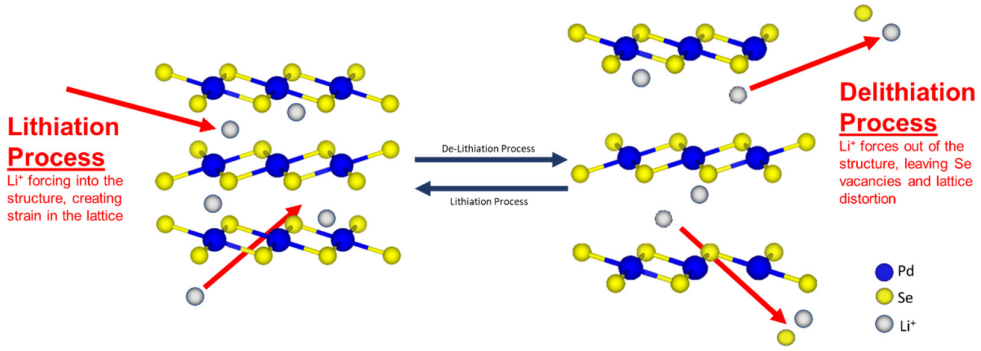

Fig. S1 Schematic illustration for synthesis of I- $PdSe_2$.

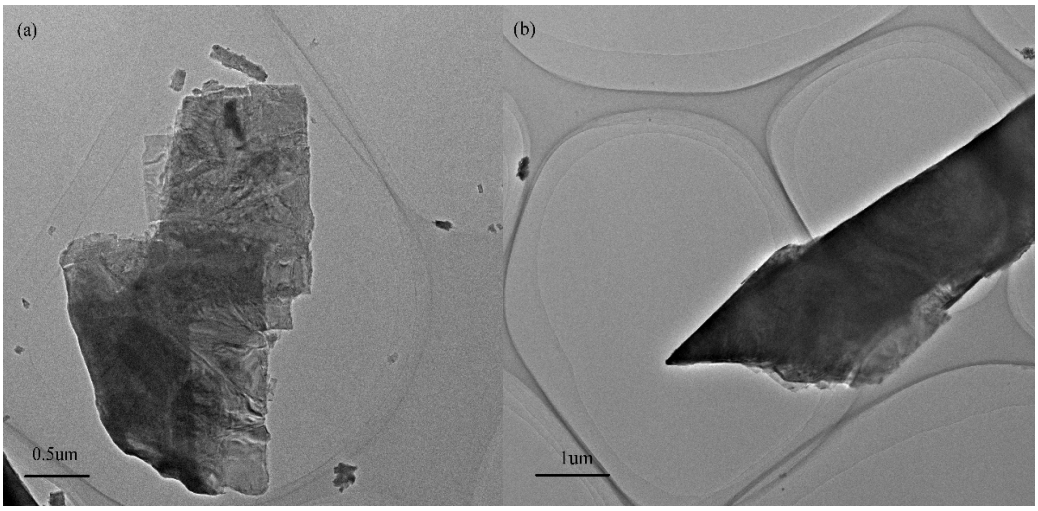

Fig. S2 TEM images (a) $PdSe_2$ (b) I- $PdSe_2$.

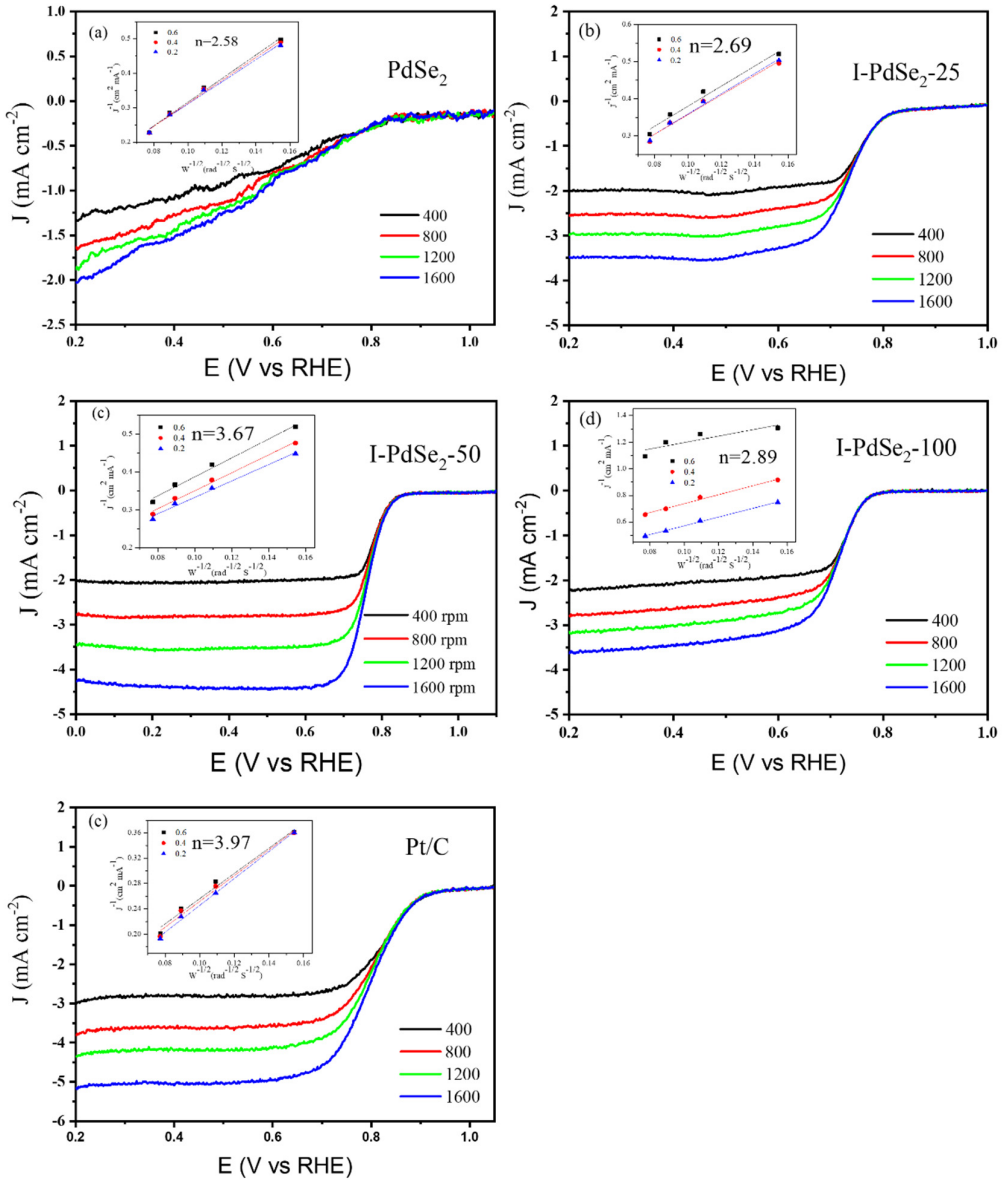

Fig. S3 LSV curves of (a) $PdSe_2$, (b) I- $PdSe_2$-25, (c) I-$PdSe_2$,(d) I-$PdSe_2$-100 and (e) Pt/C catalysts in O_2-saturated 0.1 M KOH solution at different rotation speeds with a sweep rate of 10 mV s^{-1}. Inset: Koutecky-Levich plots (i−1 Vs ω−1/2) relationship.

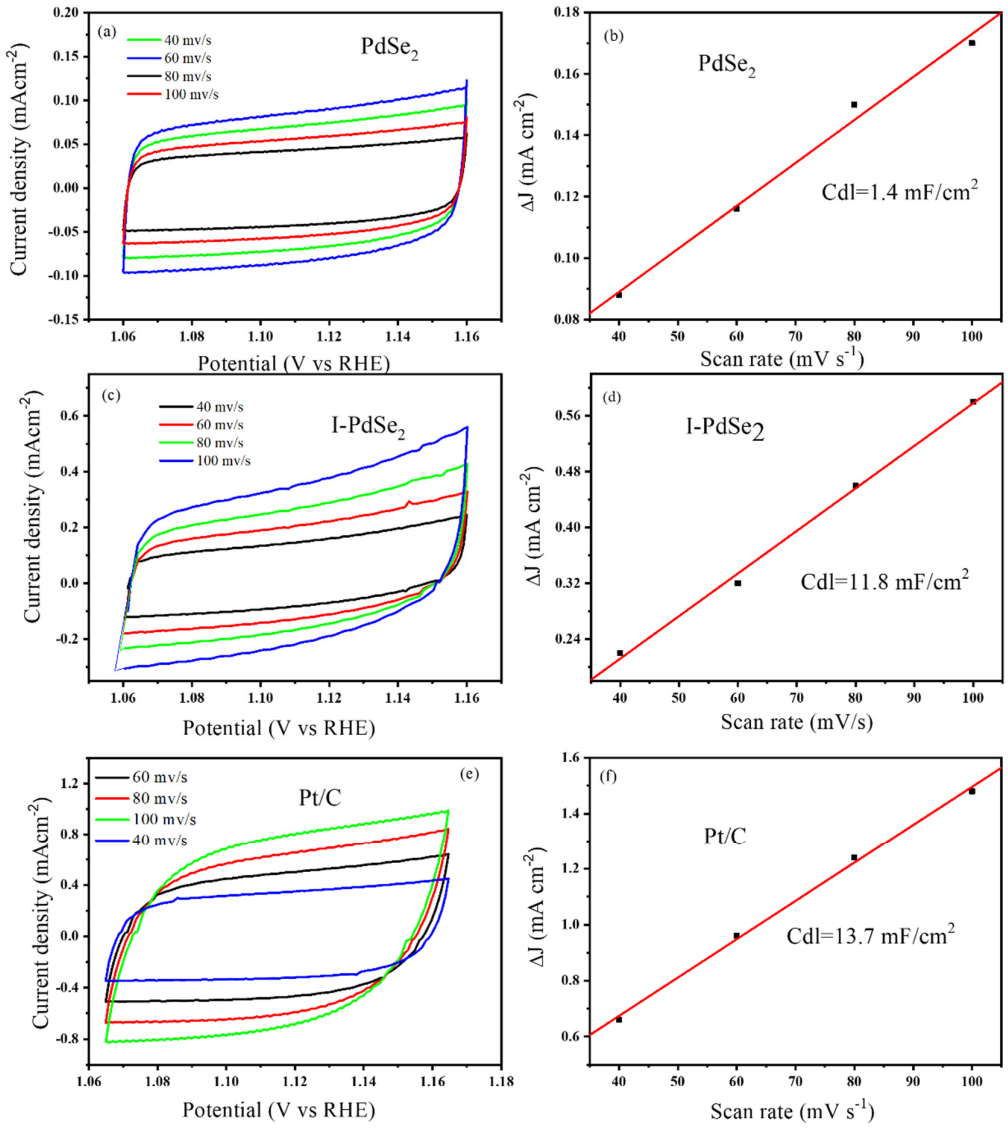

Fig. S4 CV curves in the region of 1.06-1.17 V at scan rates from 40 to 100 mV s^{-1} and corresponding linear fitting of capacitive current: (a) and (b) for $PdSe_2$; (c) and (d) for I- $PdSe_2$; (e) and (f) for Pt/C.

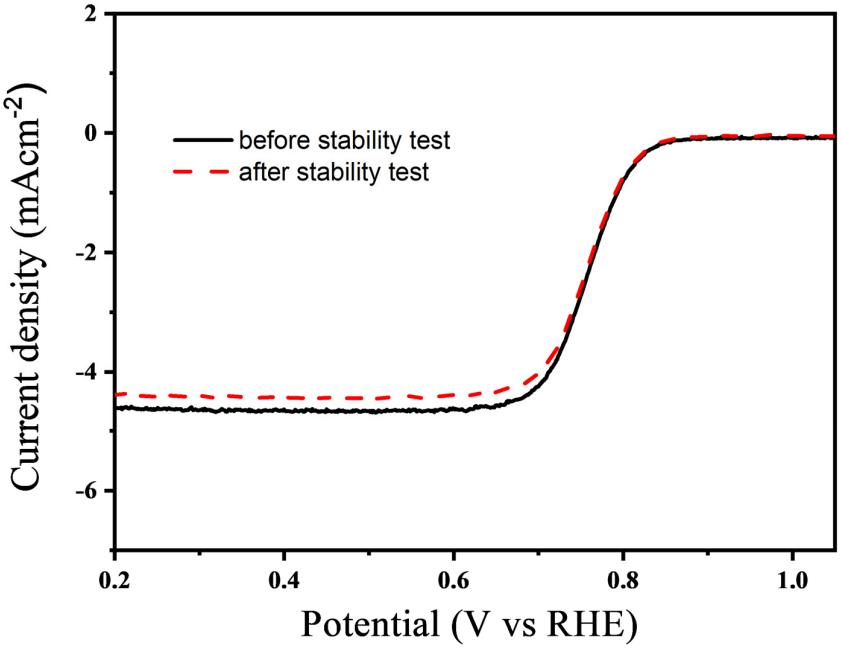

Fig. S5 LSV after 28800s Chronoamperometric test for I-$PdSe_2$.

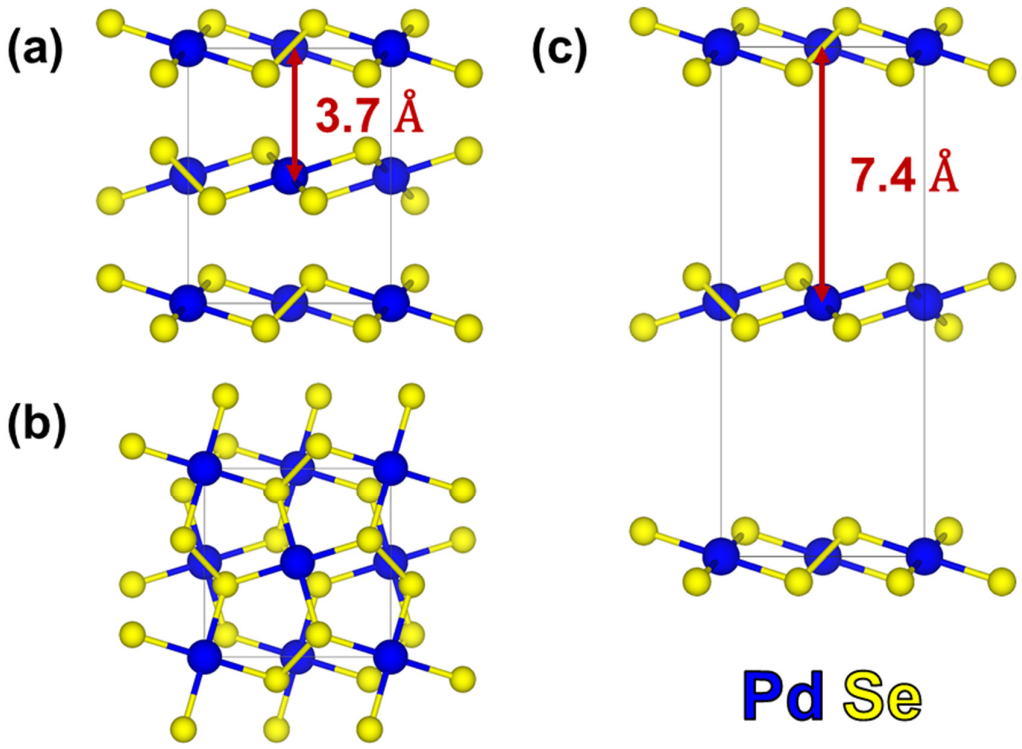

Fig. S6 Bulk structures of $PdSe_2$ and I-$PdSe_2$.

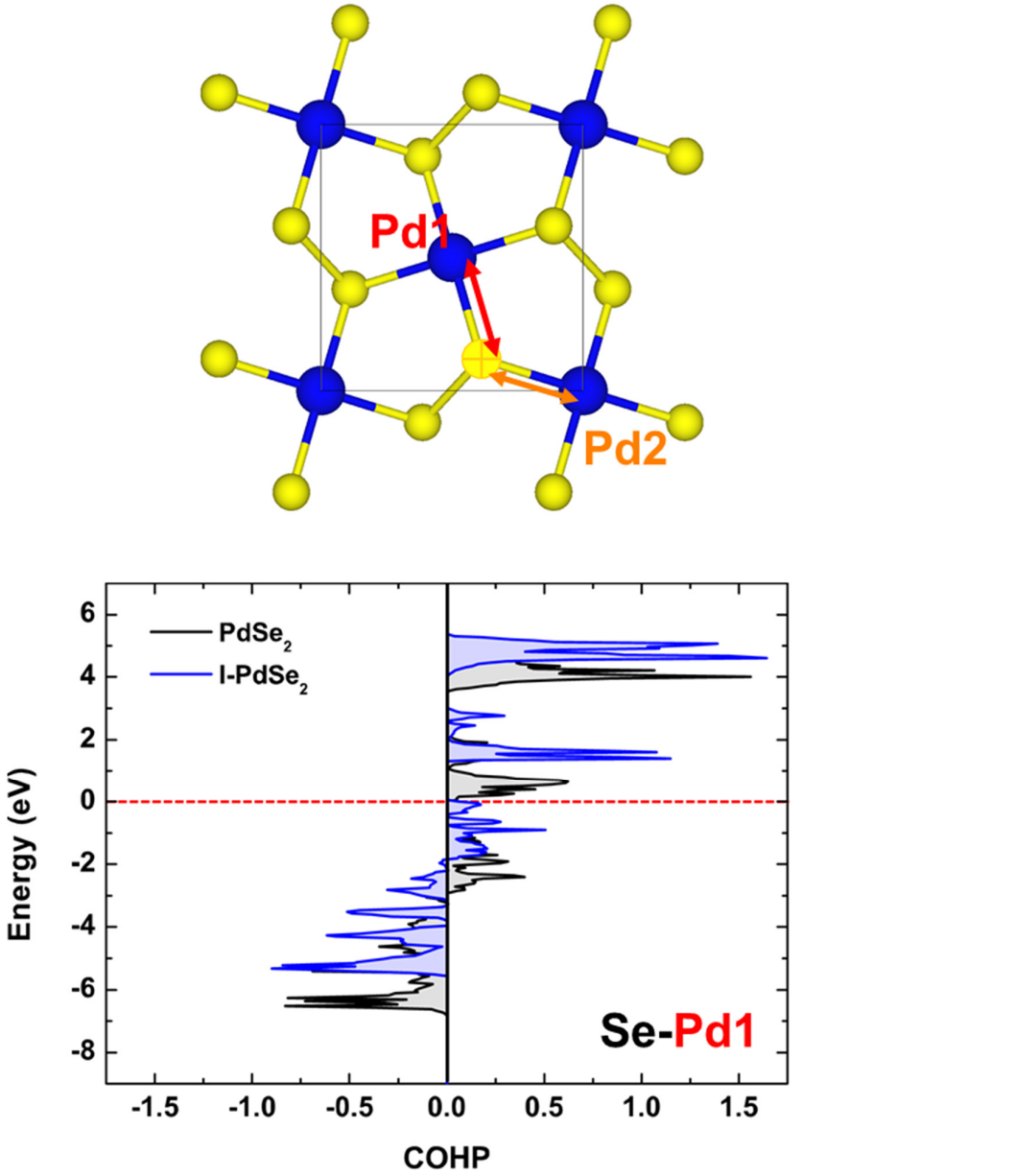

Fig. S7 COHP of the bond between Se and Pd on the surface for $PdSe_2$ (black) and I-$PdSe_2$ (blue). The Fermi energy is set to 0 eV.

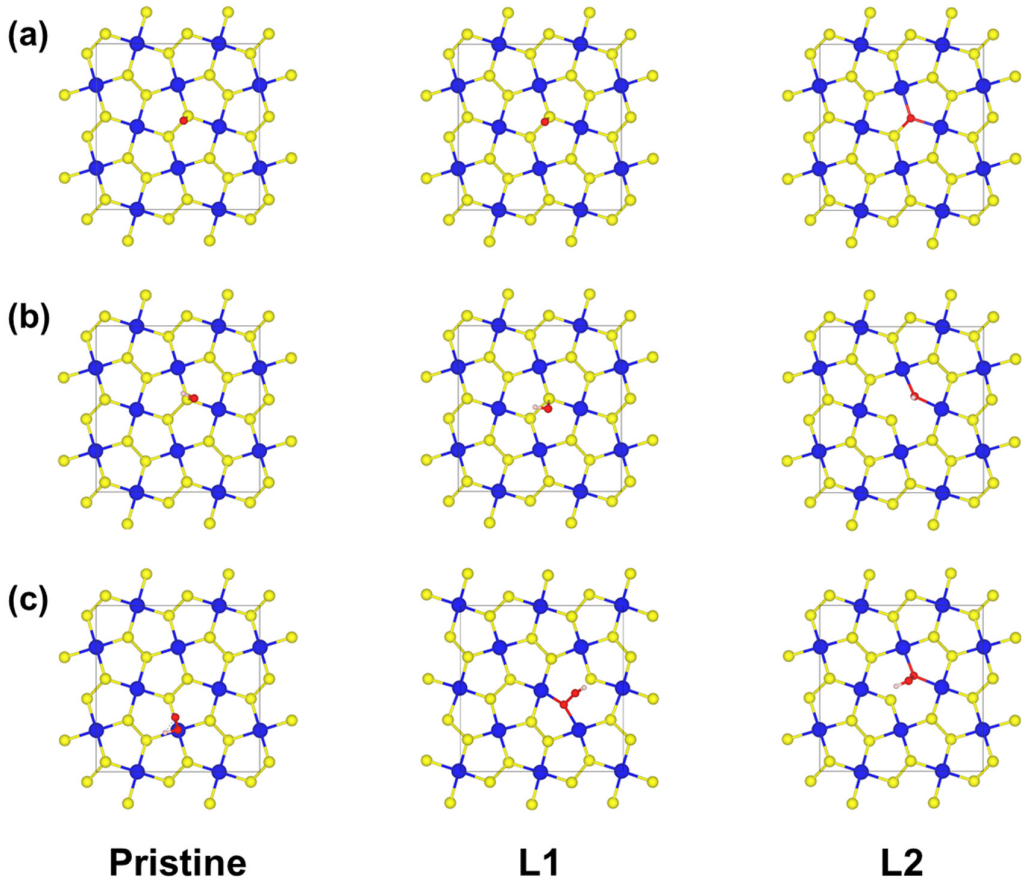

Fig. S8 Top view of the second layer (2L) for pristine and defective I-$PdSe_2$ with adsorbed intermediates (a) O, (b) OH and (c) OOH.

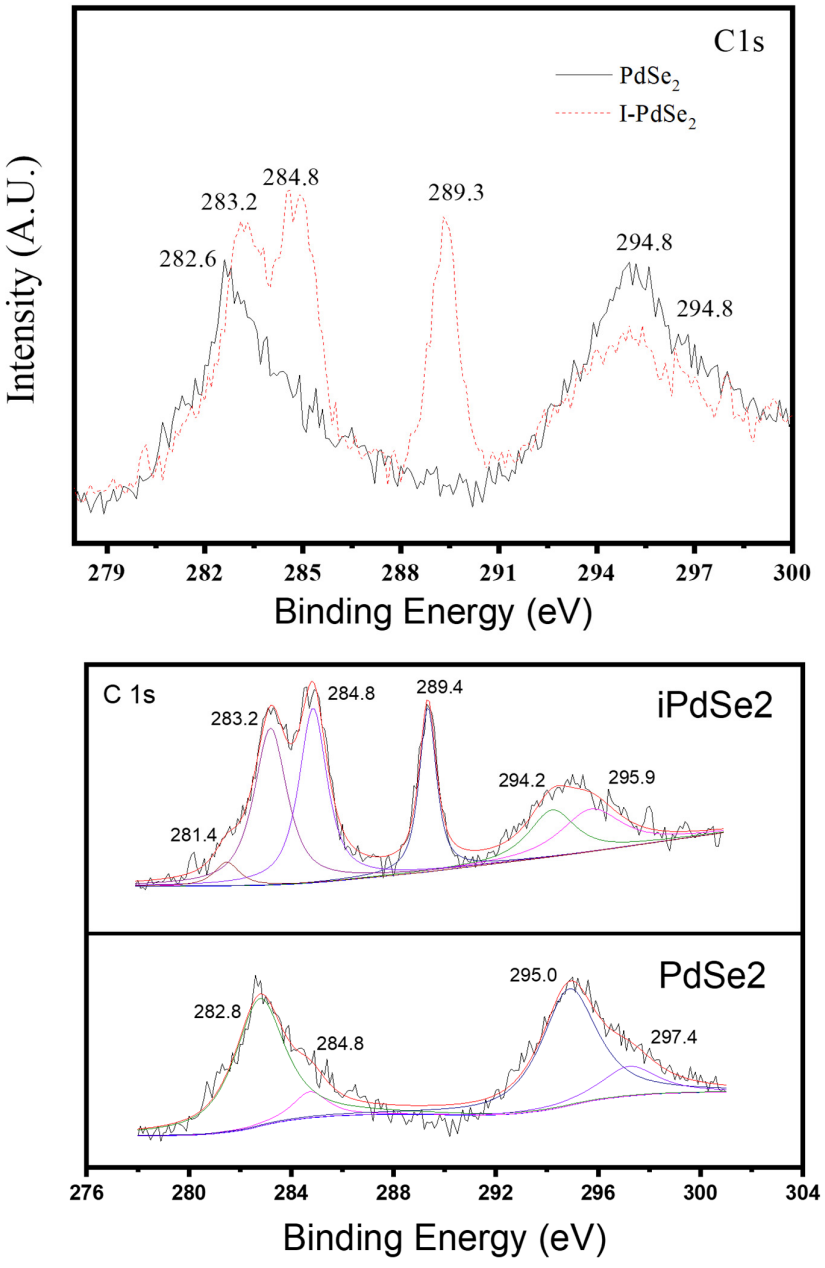

Fig. S9 XPS Carbon 1s Spectra.

	ΔG_1	ΔG_2	ΔG_3	ΔG_4
$PdSe_2$	0.353 eV	-2.582 eV	-0.718 eV	-1.973 eV
I-$PdSe_2$	0.482 eV	-2.697 eV	-0.007 eV	-2.698 eV
I-$PdSe_2$ (L1)	-1.075 eV	-2.892 eV	-0.246 eV	-0.707 eV
I-$PdSe_2$ (L2)	0.419 eV	-2.629 eV	-0.008 eV	-2.702 eV
I-$PdSe_2$ (2L)	0.318 eV	-2.524 eV	-0.347 eV	-2.366 eV
I-$PdSe_2$ (L1_2L)	0.300 eV	-2.536 eV	-0.103 eV	-2.581 eV
I-$PdSe_2$ (L2_2L)	-1.249 eV	-2.717 eV	-0.090 eV	-0.865 eV

Table. S1 Free energy change for each reaction steps of pristine and defective models with different active sites.

XRD Characterisation

The interlayer distance was estimated via the lattice's 002 peak. There is very minute change in the XRD spectrum, i.e., 0.1 degree peak shift. Hence overall, there is small change in the structure of the material. There is a noticeable decrease in the total area of the peak which may suggest less planar like structure is present, consistent with the less crystalline structure observed in TEM characterization. This phenomenon is expected from the incurrence of Se vacancies because of the invasive nature of the intercalation process.

Table. S2: fitting of 002 peak on XRD spectrum.

	I-PDSE2	**PDSE2**
FWHM	0.1686	0.1385
Peak Position	23.22	23.09449
Area	150.06131	16399.5184
Interlayer distance	0.38275 nm	0.3848 nm
Est. # layers	2.19344	2.655

	Element	At%	Se:Pd Ratio
PdSe2	Pd	37.74	1.6497
	Se	62.26	
I-PdSe2	Pd	38.66	1.5867
	Se	61.34	

Table. S3 Atomic% of Pd and Se and Se:Pd Ratio in $PdSe_2$ and I-$PdSe_2$ calculated from XPS spectrum.

Catalyst	Half-wave Potentials (V)	Mass activities ($mA\ \mu g^{-1}_{Pd}$)	Electron Transfer Number (n)
$PdSe_2$	0.58	0.030	2.58
I- $PdSe_2$-25	0.74	0.042	2.69
I- $PdSe_2$-50	0.76	0.054	3.67
I- $PdSe_2$-100	0.71	0.040	2.89
Pt/C	0.79	0.063	3.97

Table. S4 Half-wave potentials, mass activities and electron transfer number of as prepared catalysts.

Catalyst	Half-wave Potentials (V)	Mass activities ($mA\ mg^{-1}_{Pd}$)	Stability		Reference
			Δhalf-wave,j (mA cm-2) (after x cycles)	ΔE (mV) (after x cycles)	
I- $PdSe_2$	0.76	0.112	+0.2	-20	This work
Pd_3Fe NPs/CB	0.79	0.298	+0.1 (1500)	+40 (1500)	1
MoS_2/Pd	0.75	0.553	-0.2 (4000)	0 (4000)	2
Ni@Pd_3	0.75	0.098	+0.1 (3000)	-1 (3000)	3
Pd/FePt	0.7	0.067	+1.0 (10000)	0 (10000)	4
PdNiSn/NG	0.75	0.164	0 (5000)	+0.1 (5000)	5
Pd-g- C3N4	0.7	0.072	8% activity loss (40000s)	-	6
Pd-Pt /C	0.75	0.224	+0.2 (10000)	-20 (10000)	7
Pd-Fe	0.77	0.085	undetermined	undetermined	8
Pd-Co/C	0.75	0.063	undetermined	undetermined	9
Pd_2-Co alloy	0.71	0.041	undetermined	undetermined	10
Cu-Pd	0.81	0.0423	+0 (1000)	-6 (1000)	11
Pd/Ni	0.65	0.141	60% loss in ECSA (400)	-	12

Table. S5 Performance of I- $PdSe_2$ catalyst and several representative results about Pd compound from recent published works.

ICOHP	$PdSe_2$	I-$PdSe_2$
Se-Pd1	-1.027	-1.048

Table. S6 ICOHP value of the bond between Se and Pd on the surface.

Bond length	$PdSe_2$	I-$PdSe_2$
Se-Pd1	2.46 Å	2.45 Å
Se-Pd2	2.48 Å	2.47 Å

Table. S7 Bond length between Se and adjacent Pd.

References

1. T. Gunji, R. H. Wakabayashi, S. H. Noh, B. Han, F. Matsumoto, F. J. DiSalvo and H. D. Abruña, The effect of alloying of transition metals (M = Fe, Co, Ni) with palladium catalysts on the electrocatalytic activity for the oxygen reduction reaction in alkaline media, *Electrochim. Acta*, 2018, **283**, 1045-1052.
2. L.-X. Zuo, L.-P. Jiang and J.-J. Zhu, A facile sonochemical route for the synthesis of MoS2/Pd composites for highly efficient oxygen reduction reaction, *Ultrason. Sonochem.*, 2017, **35**, 681-688.
3. J. Jiang, H. Gao, S. Lu, X. Zhang, C.-Y. Wang, W.-K. Wang and H.-Q. Yu, Ni–Pd core–shell nanoparticles with Pt-like oxygen reduction electrocatalytic performance in both acidic and alkaline electrolytes, *J. Mater. Chem. A*, 2017, **5**, 9233-9240.
4. V. Mazumder, M. Chi, K. L. More and S. Sun, Core/Shell Pd/FePt Nanoparticles as an Active and Durable Catalyst for the Oxygen Reduction Reaction, *J. Am. Chem. Soc.*, 2010, **132**, 7848-7849.
5. L. Sun, B. Liao, X. Ren, Y. Li, P. Zhang, L. Deng and Y. Gao, Ternary PdNi-based nanocrystals supported on nitrogen-doped reduced graphene oxide as highly active electrocatalysts for the oxygen reduction reaction, *Electrochim. Acta*, 2017, **235**, 543-552.
6. S. K. Konda, M. Amiri and A. Chen, Photoassisted Deposition of Palladium Nanoparticles on Carbon Nitride for Efficient Oxygen Reduction, *J. Phys. Chem. C*, 2016, **120**, 14467-14473.
7. W. Wang, Z. Wang, J. Wang, C.-J. Zhong and C.-J. Liu, Highly Active and Stable Pt–Pd Alloy Catalysts Synthesized by Room-Temperature Electron Reduction for Oxygen Reduction Reaction, *Adv. Sci.*, 2017, **4**, 1600486.
8. S. Yin, M. Cai, C. Wang and P. K. Shen, Tungsten carbide promoted Pd–Fe as alcohol-tolerant electrocatalysts for oxygen reduction reactions, *Energy Environ. Sci.*, 2011, **4**, 558-563.
9. Y.-C. Wei, C.-W. Liu, Y.-W. Chang, C.-M. Lai, P.-Y. Lim, L.-D. Tsai and K.-W. Wang, The structure-activity relationship of Pd–Co/C electrocatalysts for oxygen reduction reaction, *Int. J. Hydrogen Energy*, 2010, **35**, 1864-1871.
10. W. Wang, D. Zheng, C. Du, Z. Zou, X. Zhang, B. Xia, H. Yang and D. L. Akins, Carbon-supported Pd-Co bimetallic nanoparticles as electrocatalysts for the oxygen reduction reaction, *J. Power Sources*, 2007, **167**, 243-249.
11. D. Chen, P. Sun, H. Liu and J. Yang, Bimetallic Cu–Pd alloy multipods and their highly electrocatalytic performance for formic acid oxidation and oxygen reduction, *J. Mater. Chem. A*, 2017, **5**, 4421-4429.
12. J. Zhao, A. Sarkar and A. Manthiram, Synthesis and characterization of Pd-Ni nanoalloy electrocatalysts for oxygen reduction reaction in fuel cells, *Electrochim. Acta*, 2010, **55**, 1756-1765.